Pharmaceutical Nanotechnology

Amino acid based amphiphilic copolymer micelles as carriers of non-steroidal anti-inflammatory drugs: Solubilization, *in vitro* release and biological evaluation

Pranabesh Dutta[a], Joykrishna Dey[a,*], Venkatesan Perumal[b], Mahitosh Mandal[b]

[a] *Department of Chemistry, Indian Institute of Technology, Kharagpur, West Bengal 721302, India*
[b] *School of Medical Science and Technology, Indian Institute of Technology, Kharagpur, West Bengal 721302, India*

ARTICLE INFO

ABSTRACT

Three novel amino acid based anionic amphiphilic copolymers poly(sodium *N*-acryloyl-L-valinate-*co*-alkylacrylamide) (where, alkyl = octyl and dodecyl) with either 9 or 16 mol% hydrophobic substitution were synthesized. These hydrophobically modified polyelectrolytes (HMPs), above a critical concentration, self-assemble in aqueous solution through inter-chain hydrophobic aggregation, forming micelle-like aggregates having hydrodynamic diameter in the range of 50–200 nm. The HMPs were found to undergo conformational changes with the change in solution pH, electrolyte and additive concentration, and temperature. The polymeric micelles were observed to be stable under biological conditions (pH 7.4, [NaCl] = 150 mM and temperature (37 °C)). The solubilization capacity of the polymeric micelles for six important non-steroidal anti-inflammatory drugs of different hydrophobicity was evaluated. Depending upon the hydrophobicity the solubilities of the drugs were observed to increase ca. 2–10 times in the presence of 1.0 g/L copolymers. The *in vitro* release kinetics of the loaded drug was studied under physiological pH. To explore their potential application in pharmaceutical industries hemocompatibility and cytotoxicity studies were carried out using hemolytic and MTT assay, respectively. The anionic HMPs were found to be not directly toxic to mammalian cells.
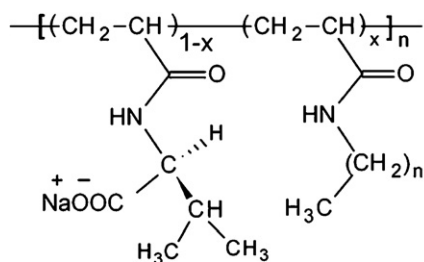
1. Introduction

In recent years there has been a tremendous interest in the field of designing drug delivery vehicles for administration of water-insoluble and toxic drugs (Farokhzad and Langer, 2009; Allen and Cullis, 2004). The hydrophobic nature of most drugs limits their efficacy and bioavailability. Therefore solubilization, encapsulation, and delivery of these drugs require water-soluble, biocompatible, and target specific drug delivery systems (DDSs) that can improve the efficacy of a drug (Kreuter, 1994; Elvira et al., 2002; Florence and Attwood, 1998; Lawrence, 1996; Uchegbu and Florence, 1995). For therapeutic applications, carriers having nanometer (∼100 nm) to submicron size (<0.4 μm) are preferred for enhanced permeability and retention (EPR) effect (Maeda et al., 2000). Another goal of drug delivery is to simultaneously increase circulation time while decreasing the dosages so that drug toxicity is reduced. A DDS not only requires sequestration and solubilization of hydrophobic drugs but also requires the ability to ultimately release the drug molecule. Thus in successful DDS, the drug cannot be tightly or chemically bound so as to prevent drug release from the delivery system.

Since the time of realization of the need for DDS different nano-size microheterogeneous systems have emerged as potential drug carriers (Kreuter, 1994). During the last twenty years or so, a variety of polymeric drug carriers (Cortesi and Nastruzzi, 1999; Cevc, 1993; Gupta and Moulik, 2008; Moulik and Paul, 1998; Tenjarala, 1999; Kantaria et al., 1999; Watnasirichikul et al., 2002) have emerged as prospective DDS. In fact, a lot of effort has been made in developing injectable, biocompatible, biodegradable polymers (Guo et al., 2005; Kakinoki et al., 2007; Okino et al., 2002) and nanoparticles (Reddy et al., 2006) for anticancer drug delivery applications. In addition, molecules with self-assembly properties have also been studied for such applications (Torchilin, 2001). The self-organizing polymeric systems often lead to enhanced therapeutic index of hydrophobic drugs through increased solubilization and modification of their pharmacokinetic profiles. The encapsulated drugs in these delivery systems are protected from degradation in biological fluids and their penetration through the biological cell membranes

* Corresponding author. Tel.: +91 3222 283308; fax: +91 3222 255303.
  E-mail address: joydey@chem.iitkgp.ernet.in (J. Dey).

Chart 1. Molecular structures of the random copolymers.

is facilitated due to the presence of interfacial lipid layer (Kunze et al., 2009). Therefore, the polymer-based drug or vaccine delivery systems have attracted much attention due to their ability to perform multiple critical functions as mentioned above.

Because they can be useful in drug delivery, the self-assembly of amphiphilic polymers (Klaikherd et al., 2009; Wittemann et al., 2007; Chelushkin et al., 2007; Yang et al., 2006; Hua et al., 2006; Garnier and Laschewsky, 2006; Gao et al., 2006), polymeric micelles (Cashion and Long, 2009; Deen and Gan, 2009; Sakai et al., 2009) and hydrophobically modified polymers (HMPs) (Obeid et al., 2009; Cavalieri et al., 2007; Min et al., 2008; Liu et al., 2007, 2010; Fan et al., 2007) in aqueous media has been investigated extensively. Recently we have also reported synthesis and aggregation behavior of three new amino acid-based hydrophobically modified anionic polyelectrolytes, poly(sodium *N*-acryloyl-L-valinate-*co*-alkylacrylamide) (see Chart 1 for structures) (Dutta et al., 2009a). Using different experimental techniques, such as surface tension, viscometry, fluorescence, electron microscopy, and dynamic light scattering it was demonstrated that the copolymers formed spontaneous unicore micelles having hydrodynamic diameter in the range of 50–200 nm with hydrophobic and viscous microenvironments. In addition, the copolymers exhibit a pH-induced conformational transition near physiological pH. These copolymers were also found to be particularly interesting in increasing the solubility of poorly water-soluble drug griseofulvin (Dutta et al., 2009b). For griseofulvin, the solubilization capacity (S_{cp}) of the HMPs was found to be ca. 11.5–27.7 mg/g, which is quite large compared to that of micelle-forming neutral surfactants [e.g., Tween 80 (3.4 mg/g), and Creomphor EL (2.6 mg/g)] and triblock copolymers ($M_n \sim$ 5000–7000 g/mol) of ethylene oxide and phenylglycidyl ether (~4.0–17.8 mg/g) (Dutta et al., 2009b). Encouraged by the preliminary results we have extended the work to other pharmaceutically active compounds. Thus in this work, the loading capacity of these copolymers for a series of hydrophobic anti-inflammatory drugs, such as (±)-fenoprofen (FNP), flurbiprofen (FLP), indoprofen (INP), ketoprofen (KTP), naproxen (NPX), and suprofen (SUP) was measured. The rational behind selecting these drugs is that they are easily available and have chromophoric groups and hence their concentration can be measured by spectrophotometric method. The drug release kinetics of two representative encapsulated drugs, NPX and KTP were studied in pH 5, and 7.4 at the physiological temperature (37 °C). The stability of the drug carriers against salt (NaCl) and additives (e.g., urea, and ethanol) was investigated. Finally, the biocompatibility of the copolymers was examined by MTT assay and hemolysis studies.

2. Experimental

2.1. Materials

The copolymers used in this study were prepared with the monomer sodium *N*-acryloyl-L-valinate (SAVal) and *N*-alkylacrylamide (alkyl = octyl and dodeyl) with either 9 or 16 mol% hydrophobic substitution in DMF solvent at 60 °C using azoisobutyronitrile (AIBN) as free radical initiator. The detailed synthetic procedure and molecular characterization could be found in our earlier report (Dutta et al., 2009a). The molecular weights and the physicochemical properties of the copolymers are summarized in Table 1. The fluorescent probes like pyrene, 1,6-diphenyl-1,3,5-hexatriene (DPH), and 1-anilinonaphthalene (AN) (Aldrich) were recrystallized from ethanol or acetone–ethanol mixture three times before use. The non-steroidal anti-inflammatory drugs (NSAIDs), (±)-fenoprofen (FNP), flurbiprofen (FLP), indoprofen (INP), ketoprofen (KTP), naproxen (NPX), and suprofen (SUP), were purchased from Sigma–Aldrich and were used as received. MTT (3-(4,5-dimethyl-2-thiazolyl)-2,5-diphenyl-2H-tetrazolium bromide) was purchased from Sigma–Aldrich (St. Louis, MO, USA). All the reagents and solvents specially dimethylformamide (DMF), ethanol, methanol, tetrahydrofuran (THF), acetone, dichloromethane were of commercially available [reagent grade (>98%)] and dried and distilled fresh before use. Sodium chloride, potassium chloride, sodium dihydrogen phosphate, and sodium hydroxide were of analytical grade and were procured from SRL, Mumbai. Double distilled water was used for preparation of all solutions.

2.2. General methods

The pH measurements were conducted with a digital pH meter Model pH 5652 (EC India Ltd., Kolkata) using a glass electrode. The UV–visible spectra were recorded in a Shimadzu (model 1601) spectrophotometer. Fluorescence spectra of 1-anilinonaphthalene (AN) probe were obtained with a Perkin Elmer LS-55 spectrofluorometer. The AN solutions were excited at 340 nm and emission was collected in the range 360–550 nm. Steady-state fluorescence anisotropy (r) of DPH was measured on the same Perkin Elmer LS-55 spectrophotometer equipped with filter polarizers that used the L-format configuration. The correction factor and the anisotropy value were determined automatically using existing software supplied by the manufacturer. The final concentration of DPH was adjusted to (2×10^{-7} M) by adding appropriate amount of ethanol stock solution of the probe. The excitation wavelength was set at 350 nm and the emission was monitored at 450 nm using excitation and emission slits with a band-pass of 2.5 and 2.5–5.0 nm, respectively. A 430 nm emission cut-off filter was used to reduce scattered and stray radiation. The temperature of the samples was set at 30 °C using the water jacketed magnetically stirred cell holder in the spectrometer connected to Thermo Neslab RTE-7 circulating water bath that enables the temperature control of ±0.1 °C.

The dynamic light scattering (DLS) experiments were performed on a Zetasizer Nano ZS (Malvern Instrument Laboratory, Malvern, U.K.) instrument employing a He–Ne laser operated at 4 mW (λ_o = 632.8 nm), and a digital correlator. Prior to the measurements, each solution was cleaned by centrifuging at a speed of 5000 rpm for 15 min followed by filtration through a 0.45 μm filter paper (Millipore Millex syringe filter). The scattering intensity was measured at a 173° angle to the incident beam. The final solution was loaded into an optical quality cylindrical quartz sample cell which subsequently placed in the DLS optical system for 30 min to equilibrate at the desired temperature (25 °C). The data acquisition was carried out for 2 min and each experiment was repeated at least two times. The apparent diffusion coefficients (D_{app}) were calculated by cumu-

Table 1
Molecular weight, polydispersity index (M_w/M_n), pK_a, critical aggregation concentration (CAC), polarity parameters (I_1/I_3), microviscosity (η_m), mean hydrodynamic radius $\langle R_h \rangle$, and zeta-potential (ζ) of 1.0 g/L SAVal-DA(0.09), SAVal-DA(0.16), and SAVal-OA(0.16) in aqueous phosphate buffer solution (pH 8).

Copolymer	M_n ($\times 10^{-5}$)(g/mol)	M_w/M_n	CAC ($\times 10^4$)(g/L)	I_1/I_3	η_m(mPa s)	$\langle R_h \rangle$ (nm)	ζ(mV)	pK_a	T_m (°C)
SAVal-DA(0.09)	2.3	1.76	45.0	1.3	44.4	54.0	−19.2	6.0	36.4
SAVal-DA(0.16)	11.7	1.15	9.0	1.0	94.0	42.0	−14.6	6.2	39.7
SAVal-OA(0.16)	11.8	1.21	220.0	1.3	73.0	11.0, 102.5	−17.6	6.1	36.8

lant analysis (first order) of an autocorrelation function generated by the scattered light intensity fluctuations. Average hydrodynamic diameter (d_h) was estimated from diffusion coefficients, using the Stokes–Einstein equation:

$$D_{app} = \frac{k_B T}{3\pi\eta d_h} \tag{1}$$

where k_B is the Boltzmann constant, T is the absolute temperature, and η is the viscosity of the solvent.

The surface zeta potential of the copolymers was also measured using Zetasizer Nano ZS (Malvern Instrument Laboratory, Malvern, U.K.) optical system equipped with an He–Ne laser operated at 4 mW ($\lambda_o = 632.8$ nm) at 25 °C. The concentrations of the copolymers were kept at 1 g/L with either pH 5/7.4 (50 mM PBS). For each sample, an average value of three successive measurements was considered.

2.3. Solubilization studies

Solubilization studies were carried out following our previous report (Dutta et al., 2009b). Briefly, the NSAIDs were dissolved in chloroform in screw-caped test tube. After complete dissolution of drug molecule, chloroform was evaporated by passing N_2 gas through it. A 5 mL polymer solution (ca. ∼0.05–2.0 g/L) was added subsequently to the tube and the polymer solution containing the drug left under stirring for five days at 37 °C to ensure the solubilization equilibrium. The insoluble drugs were removed by centrifugation at a speed of 4000 rpm for 10 min followed by careful filtration of the supernatant using Millipore Millex filter (0.45 μm pore diameter). An aliquot of these samples was diluted with methanol and absorbance value was measured by a UV–vis spectrophotometer at an analytical wavelength (see Table 2) using the previously recorded calibration curve. The copolymer solution at the same dilution was used as a blank. The same procedure was also applied for every single drug molecule to determine their water solubility and make necessary correction. Solubilization capacities (S_{cp}) and encapsulation efficiency (E_{ef}) were calculated for 1 g/L copolymer solution according to the following equations (Yalkowsky, 1999; Miguel et al., 2008):

$$S_{cp} \text{(mg/g)} = \frac{(S_{poly}^G - S_{water}^G)}{(C_{poly} - \text{CAC})} \tag{2}$$

$$E_{ef} = \frac{\text{amount of drug encapsulated in polymer (mg)} \times 100}{\text{amount of drug added (mg)}} \tag{3}$$

where S_{poly}^G is the solubility of drug in copolymer solution (mg/L), S_{water}^G is the solubility of drug in water (mg/L), C_{poly} is the concentration of the copolymer in g/L (1.0 g/L), and CAC is the critical aggregation concentration of the copolymer.

2.4. Drug release kinetics

In vitro drug release kinetics was performed with KTP- and NPX-loaded drug solution in both pH 5 and pH 7.4 at 37 °C for 1 g/L copolymer solution. The dialysis was carried out with 1 mL solution of drug-loaded polymer micelles from the double sided Biodialyzer (Aldrich) dialysis compartment using cellulose membrane

with molecular weight cutoff of 12 kDa. Before every measurement, un-entrapped drug was removed from the solution by dialyzing against 20 mL buffer solution of pH 5 in a 2 h of dialysis, the dialysis cell was withdrawn and immediately maintained into a freshly prepared buffer solution and dialyzed against buffer of the desired pH (pH 5.0: acetate; pH 7.4: phosphate, 0.1 M NaCl) at 37 °C. At intervals, aliquots of 2 mL were withdrawn from the solution to quantify the amount of release from the micelles. The volume removed from the dialysis cell was replaced by adding 2 mL fresh buffer solution after each sampling to ensure sink conditions.

2.5. Hemolytic assay

The copolymers were dissolved in sterile water to desired concentrations (0.1 g/L and 1 g/L). Hemolytic assay was performed using the protocol reported by Katanasaka et al. (2008) with some modification. In brief, blood was obtained from 6-week-old BALB/c male mice and red blood cells (RBCs) were collected by centrifugation (1500 rpm, 5 min, and 4 °C) of the blood. The collected RBC pellet was diluted in 20 mM HEPES buffered saline (pH 7.4) to give a 5%(v/v) solution. The RBC suspension was added to HEPES–buffered saline, 1% Triton X-100, and samples and incubated for 60 min at 37 °C. After centrifugation with (Heraeus table top centrifuge 5805R) at 12,000 rpm at 4 °C, the supernatants were transferred to a 96-well plate. Hemolytic activity was determined by measuring the absorption at 550 nm using benchmark microplate reader (Biorad Microplate reader 5804R). The samples with 0% lysis (HEPES buffer saline) and 100% lysis (1% Triton X-100) were referred as [+]ve and [−]ve control, respectively. All assays were performed in triplicate. Hemolytic activity of each treatment was expressed as percent cell lysis relative to the untreated control cells (% control) is defined as:

hemolysis (%)

$$= \frac{(\text{abs at } 550 \text{ samples} - \text{abs at } 550 \text{ }^-\text{ve control})}{(\text{abs at } 550 \text{ }^+\text{ve control} - \text{abs at } 550 \text{ }^-\text{ve control})} \times 100 \tag{4}$$

2.6. In vitro cytotoxicity assay

Fibroblast cell 3T3 cell line (frozen three months before) was grown in RPMI-1640 medium supplemented with 10% FBS, 2 mM L-glutamine, 100 units/mL penicillin, and 0.1 mg/mL streptomycin. Cells were grown in T-25 flasks at 37 °C, 5% CO_2 with a feeding cycle of 2 days. After cells became 80% confluent (after 2 days) they were trypsinized (0.25% trypsin + 0.1% EDTA), centrifuged and were suspended in RPMI 1640. Cells were seeded in fresh T-25 flasks at a density of 3×10^3 cells/cm² and were cultured in RPMI 1640 with a feeding cycle of 2 days.

The copolymers were dissolved in sterile water (pH 7.4) and filtered through 0.2 μm polycarbonate filter. Then the samples were diluted to desired concentrations. Cell suspensions were seeded into a 96-well plate at a density of 3×10^3 cells/well in 0.1 mL complete medium. The cells were allowed to adhere and grow for 24 h at 37 °C in an incubator (Heraeus Hera Cell), after which the medium was aspirated and replaced with 0.1 mL fresh medium containing control and samples with the desired concentrations. After

Table 2

Physicochemical properties and solubility in water, solubility (S_{eq}) (mg/L), solubilization capacity (S_{cp}) (mg/g), and encapsulation efficiency (E_{ef}) (%) of KTP, INP, SUP, FNP, NPX, and FLP in pH 5 for 1.0 g/L SAVal-DA(0.09), SAVal-DA(0.16), SAVal-DA(0.16) copolymers.

Drugs	[a]λ(nm)	[b]$\log K_{ow}$	[c]ε(L mol^{-1} cm^{-1})	[d]Solubility(mg/L)	Copolymers	Solubilization parameters		
						S_{eq}	S_{cp}	E_{ef}
KTP	256	2.683	16,367	510 (490)	SAVal-DA(0.09)	1394 ± 132	887	7.8
					SAVal-OA(0.16)	1683 ± 167	962	11
					SAVal-DA(0.16)	2363 ± 122	1853	14.1
SUP	295	2.659	15,384	560	SAVal-DA(0.09)	1670 ± 154	1110	11.2
					SAVal-OA(0.16)	1927 ± 113	1365	13.3
					SAVal-DA(0.16)	2952 ± 201	2389	21.6
INP	283	2.391	12,398	77	SAVal-DA(0.09)	871 ± 119	798	43.4
					SAVal-OA(0.16)	962 ± 115	887	57.6
					SAVal-DA(0.16)	1672 ± 179	1596	72.3
NPX	271	2.998	4231	22 (16, 25)	SAVal-DA(0.09)	131 ± 11	114	18.9
					SAVal-OA(0.16)	147 ± 14	131	21.8
					SAVal-DA(0.16)	234 ± 13	218	47.1
FNP	271	3.449	2649	13	SAVal-DA(0.09)	113 ± 10	101	27.5
					SAVal-DA(0.16)	134 ± 15	122	39.5
					SAVal-DA(0.16)	199 ± 9	187	56.3
FLP	247	3.769	19,526	11	SAVal-DA(0.09)	124.5 ± 13.2	112	30.3
					SAVal-OA(0.16)	167.4 ± 15.4	156	41.4
					SAVal-DA(0.16)	205.4 ± 11.4	194	63.2

[a] Analytical wavelength used for quantification.
[b] Octanol–water partition coefficient.
[c] Molar extinction coefficient.
[d] Aqueous solubility (the data in the parentheses are reported value) [Péhourcq et al., 2001; Leo et al., 1971].

48 h, the culture medium was removed and the cells were washed with sterile phosphate buffer saline (PBS) (0.1 mL/well) three times. Cell viability was assessed using a conventional MTT (3-(4,5-dimethyl-2-thiazolyl)-2,5-diphenyl-2H-tetrazolium bromide) dye reduction assay. 0.1 mL of MTT reagent in PBS (1 g/L) was added to each well. After 4–5 h incubation, the MTT reagent mixture was gently removed and 0.1 mL DMSO was subsequently added into each well to dissolve the purple formazan precipitate which was reduced from MTT by the viable cells with active mitochondria. The formazan dye was measured spectrophotometrically using benchmark microplate reader at 550 nm. All assays were performed in triplicate. The cytotoxic effect of each treatment was expressed as percent cell viability relative to the untreated control cells (% control) defined as:

$$\text{cell viability (\%)} = \frac{(\text{absorbance at } 550 \text{ of treated cells with samples})}{(\text{absorbance at } 550 \text{ of control cells without samples})} \times 100 \quad (5)$$

2.7. Statistical analysis

The statistical method used to analyze the significant differences between control and treatment groups is one-way analysis of variance (ANOVA). The results were expressed as mean ± SD unless otherwise noted; ***$p < 0.001$ was considered statistically significant.

3. Results and discussion

3.1. Physicochemical properties of HMPs

The detailed solution behavior of the HMPs employed in this study has been reported in our earlier publication (Dutta et al., 2009a). A summary of the physicochemical properties of the copolymers has been presented in Table 1. The data in Table 1 suggest that the HMPs have high molecular weights in the range

of 200–1000 kDa. The copolymers SAVal-DA(0.16) and SAVal-OA(0.16), however, have narrow molecular weight distributions. All these HMPs form aggregates above CAC. The HMP with higher hydrophobe content has lower CAC value. On the other hand, decrease of hydrophobic chain length increases the CAC value. The aggregates in solutions of SAVal-DA(0.09) and SAVal-DA(0.16) have average size around 50 nm. On the other hand, SAVal-OA(0.16) exhibits existence of two types of aggregates, one having average hydrodynamic radius ($\langle R_h \rangle$) ca. 10 nm and the other having R_h of about 100 nm. The nanosize aggregates thus formed have overall negative charges as indicated by the negative zeta-potential (ζ) values. The values of polarity parameters (I_1/I_3) suggest that the microenvironments of the polymeric nanoparticles are less polar compared to bulk water (1.69) (Khatua and Dey, 2007), showing their ability to solubilize hydrophobic molecules. However, the microenvironments of the nanoparticles are very viscous compared to normal micelles of ionic surfactants. This is indicated by the large values of η_m which were obtained from steady-state and time-resolved fluorescence studies. The pK_a value corresponding to the protonation of the –COO$^-$ group of the nanoparticles is ca. 6.0, suggesting conformational changes around pH 6.0 upon acidification of the aqueous solution. The melting temperatures of the nanoparticles are close to physiological temperature (37 °C).

3.2. Solubilization of NSAIDs

The NSAIDs are the analgesics and anti-inflammatory pharmaceutical compounds most commonly used for symptoms associated with osteoarthritis and other chronic musculoskeletal conditions across the world (Marie, 1998). They are used mainly to treat pain, inflammation and fever in animal and human species. However, poor solubility of NSAIDs restricts their use in topical and parenteral applications. In order to improve the solubility of NSAIDs in water, addition of surface-active agents and formation of water-soluble salts have been used earlier (Yumiko et al., 1996; Makiko et al., 2000). Among others, NSAIDs with propionic acid classes ($pK_a \sim 3–5$) are found to be particularly interesting in medical application. Although, the sodium salt forms of these drugs are

more soluble in water and used for drug formulation, they have very limited solubility in pH close to their pK_a (~4–5) (Hadgraft et al., 2000; Yiyun and Tongwen, 2005). Therefore, in this study, the solubility of six most important and commonly used NSAIDs of different hydrophobicity has been measured at different concentrations (above CAC) of SAVal-DA(0.09), SAVal-OA(0.16), and SAVal-DA(0.16) in pH 5. The solubilization of the drugs into the miceller aggregates of the copolymers was achieved by direct dissolution method in the concentration range 0.05–2.0 g/L. The amount of the drug loaded at equilibrium was determined spectrophotometrically at an analytical wavelength of the drug molecules. The solubilities of some NSAIDs in pure water were obtained from literature (Fini et al., 1995; Hadgraft et al., 2000). The solubility of other NSAIDs in pure water was determined by the above procedure. The solubility data along with some physicochemical properties of the NSAIDs have been collected in Table 2. To further evaluate the efficacy of the system in solubilization, two important parameters, solubilization capacity (S_{cp}), and encapsulation efficiency (E_{ef}) (i.e., the % of drug incorporated into the micelles) described above in the experimental section were estimated using 1.0 g/L copolymer solution.

The plots of equilibrium solubility (S_{eq}) of the NSAIDs at different concentrations of the copolymers are shown in Fig. 1. Obviously, the aqueous solubilities of NSAIDs increased linearly over the range of polymer concentration. To compare the enhancement in solubility for a given copolymer against all the drugs the S_{eq}/S_w i.e., the solubility enhancement factor was calculated. The S_{eq}/S_w values for all the three copolymers have been shown as bar graph in Fig. 1. It can be seen that the S_{eq}/S_w value for any individual NSAID increases for the copolymer in the order SAVal-DA(0.16) > SAVal-OA(0.16) > SAVal-DA(0.09). It is well known that the enhancement in solubilization of any compound depends not only on the hydrophobicity of the hydrophobic solute it is also a strong function of the internal environment of the solubilizate. The fluorescence probe data described in Table 1 suggest that in 1 g/L polymer solution, the micropolarity and microviscosity of the copolymers SAVal-DA(0.09), and SAVal-OA(0.16) are 1.32 and 44.4 mPa s, and 1.34 and 73.6 mPa s, respectively. Therefore, they have almost comparable hydrophobic character. In comparison, the copolymer SAVal-DA(0.16) has less polar and more viscous microenvironment reflected by its low I_1/I_3 (~1.02) and high η_m (~94.0) values. Therefore, it is quite reasonable that the partitioning would be more favored in case of more hydrophobic copolymer SAVal-DA(0.16).

The solubilities in copolymer solution and in pure water (Table 2) were further compared among the NSAIDs, and it is observed that the smallest enhancement in solubilization obtained for the drugs KTP and SUP. Thus in presence of 1 g/L SAVal-DA(0.09) copolymer the solubilities for KTP and SUP are 1394 and 1670 mg/L, respectively, which are ca. 1.8 and 3.0 times enhancement relative to their aqueous solubility. Under the same concentration, the solubilities of KTP in SAVal-OA(0.16), and SAVal-DA(0.16) are, however, 1683 and 2363 mg/L which are ca. 2 and 3 fold increase, respectively. On the other hand, the solubilities of SUP in the same polymer solutions are 1927 and 2952 mg/L, which are ca. 3 and 5 fold increase, respectively. From Table 2, it is observed that the KTP and SUP have nearly the same octanol/water partition coefficient, log K_{ow} value (Table 2), and their water solubilities are higher compared to the other NSAIDs. Because of their hydrophilic character they prefer to remain in bulk water. Hence, the partitioning into the hydrophobic microenvironment is comparatively less for these two drug molecules. NPX and FNP, on the other hand, have very low water solubility (~22 and 13 mg/L, respectively) and high log K_{ow} value. As a result, the solubility is greatly enhanced for these two drugs in presence of the copolymers.

However, surprisingly the solubility of INP (less hydrophobic and more water soluble than FNP, and NPX) showed a huge increase of solubility in presence of the HMPs. Thus, while SAVal-DA(0.09) and SAVal-OA(0.16) increase their solubility ca. 11, and ca. 13 times, respectively, the copolymer SAVal-DA(0.16) increases almost 22 times, which is the largest enhancement among all the drugs employed. If one closely looks at the molecular structure of INP, it can be found that it has one tertiary amine group, which in pH 5 probably gets protonated and carries an overall positive charge. On adding to copolymer solution, along with the hydrophobic interaction it also interacts with the carboxylate groups that remain dissociated at that pH through electrostatic interaction.

3.3. In vitro drug release

In order to investigate *in vitro* drug release, KTP and NPX were chosen arbitrarily as representative examples. The release studies were carried out for KTP and NPX loaded copolymer micelles in 1.0 g/L SAVal-DA(0.16). Fig. 2 presents the release profiles of the drugs in pH 5.0 and 7.4 at 37 °C. As observed, the KTP-loaded micelles at pH 5.0 showed much faster drug release kinetics than NPX-loaded micelles, which is due to the increased aqueous solubility and weak hydrophobic interaction between KTP and hydrophobic inner core of the micelles. Thus, while for KTP almost 100% release was achieved within 12 h, more than 45 h was taken to attain the equilibrium in case of NPX. When the same was compared in pH 7.4, it was observed that unlike low pH the release is comparatively faster even in case of NPX drug. The cumulative release data (%) were further analyzed using Korsmeyer–Peppas power law model ($M_t/M_\infty = kt^n$) (Ritger and Peppas, 1987) to study the mechanism of drug release kinetics. A good correlation coefficient ($R^2 = 0.99$) was observed for both KTP and NPX. The resulting release exponent value (n) < 0.5 confirmed diffusion based drug release mechanism for this polymeric system (Dutta et al., 2009b). For both the drugs, it was observed that the kinetic constant k decreased upon increase of pH from 5.0 to 7.4 suggesting faster release (about 1.5 times) at pH 7.4.

3.4. Evaluation of micelle stability against additives

The stability of the polymeric micelles is one of the major concerns for pharmaceutical application. To evaluate the same we have earlier investigated the influence of pH and temperature on the dissociation of micelles at different polymer concentrations. It was observed that at low pH < 6.0 the micelles become compact and rigid due to the loss of polyelectrolyte character and they dissociate slowly at low polymer concentration above 37 °C. However, at high polymer concentration (~1.0 g/L) these have enough stability for drug delivery application. Here, we investigate the influence of different organic and inorganic additives, for example, ethanol, urea, and salt (NaCl). The effects of additives on the stability of the polymeric micelles were studied by steady state fluorescence probe technique using AN, and DPH as extrinsic probe molecules. It is known that AN when solubilized in nonpolar environment exhibits a large shift of the fluorescence emission maximum ($\Delta\lambda$) accompanied by a huge increase of fluorescence intensity relative to that in water (Kujawa et al., 2006). On the other hand, fluorescence anisotropy (r) of DPH probe gives an idea about the rigidity of it microenvironment (Repáková et al., 2004). We therefore measured $\Delta\lambda$ value of AN and r-value of DPH probe in 0.25 g/L and 1.0 g/L polymer solutions in the presence of different concentrations of urea. Fig. 3 shows the plots of $\Delta\lambda$ and r as a function of [urea]. As seen from the figure, in concentrated solution (1.0 g/L) of the polymers, there was hardly any change of the fluorescence properties of AN and DPH probes upon addition of increasing con-
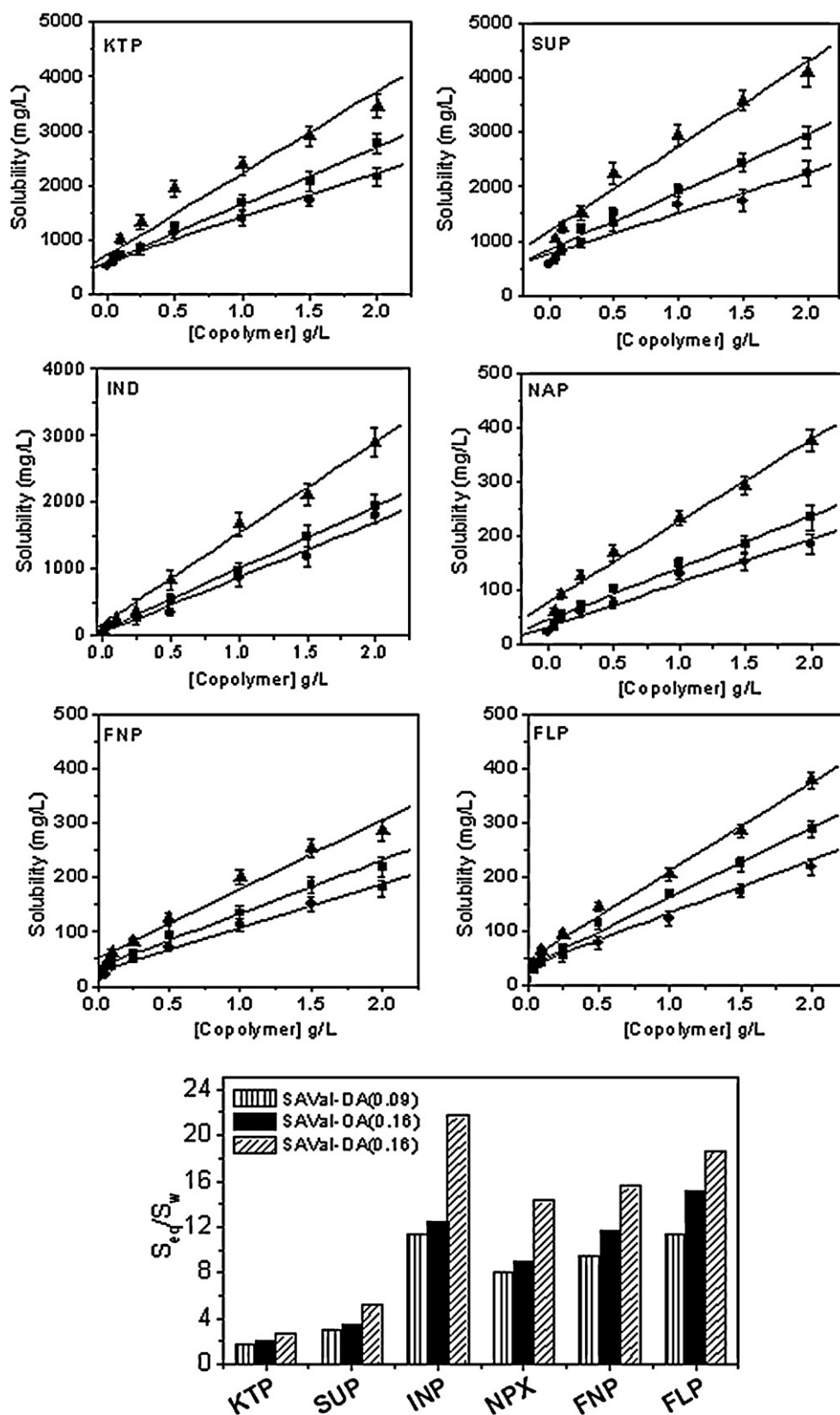
Fig. 1. Solubility profiles of NSAIDs in the presence of anionic HMPs in aqueous buffer solution (pH 5, 100 mM NaCl); (●) SAVal-DA(0.09), (■) SAVal-OA(0.16), and (▲) SAVal-DA(0.16); bar diagram showing the solubility enhancement factor (S_{eq}/S_w) of NSAIDs measured in 1.0 g/L HMP solution.
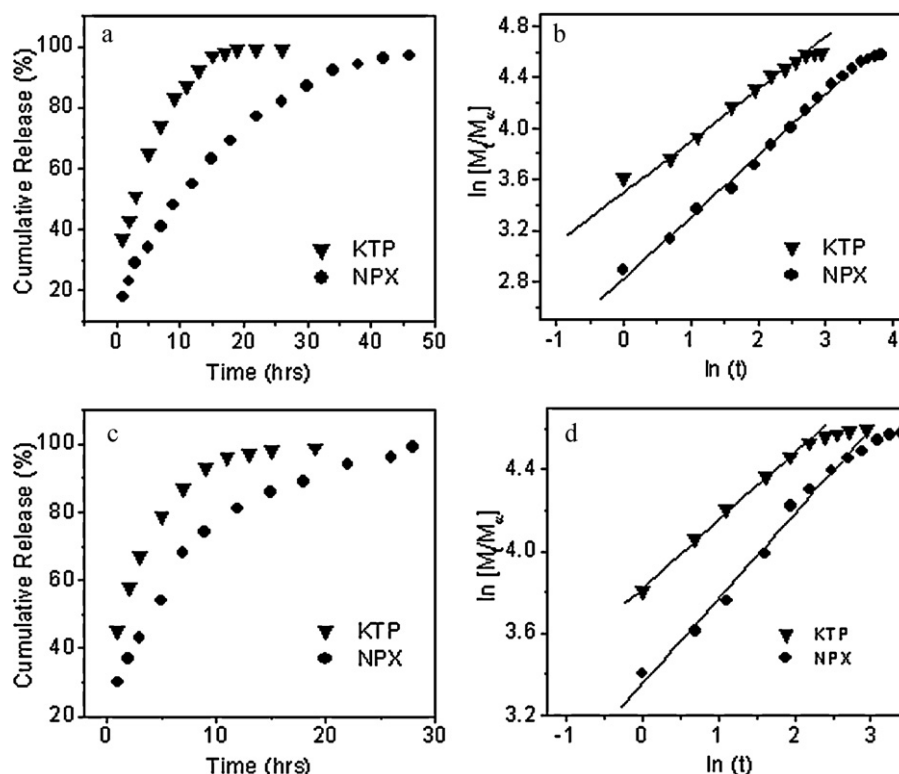
Fig. 2. The release profiles of KTP and NPX from SAVal-DA(0.16) copolymer micelles with 0.1 M NaCl at 37 °C; (a) pH 5, and (c) pH 7.4; plots of ln [M_t/M_α] versus ln t for KTP and NPX; (b) pH 5, and (d) pH 7.4.

centration of urea. This is because in concentrated solution, the polymeric micelles are very compact and urea molecules are unable to penetrate them. However, in 0.25 g/L polymer solution, both $\Delta\lambda$ and r-value decreased with the increase of [urea], indicating desta-bilization of the aggregates, which releases the probe molecules to the bulk solvent. It can be seen that the $\Delta\lambda$ value is very small even in the presence of 8 M urea, suggesting that the polarity of water has not changed significantly. This means that the urea molecules penetrate into the hydrophobic domain thus increasing the micro-polarity of the aggregates which is also indicated by the increase of hydrodynamic volume of the aggregates. Fig. 4 shows the size dis-tributions of the polymeric micelles in 0.25 g/L SAVal-DA(0.09) and SAVal-DA(0.16) in the presence of different concentrations of urea. It is interesting to see that although a single narrow size distribution was observed in aqueous solution of SAVal-DA(0.16), in the pres-ence of 2 M urea a new peak corresponding aggregates with average diameter ca. 10 nm appears. However, it is clear from the figure that the size distributions gradually shift toward larger diameter range

with the increase of urea concentration, suggesting destabilization of the aggregates.

In order to study the effect of ethanol on the micelle stability, fluorescence anisotropy of DPH probe was measured in the pres-ence of varying ethanol concentration (5–70% v/v) for two different polymer concentrations (0.25 g/L and 1.0 g/L). The plot of the vari-ation of r as a function of [EtOH] is shown in Fig. 5. As observed, at low polymer concentration, the r-value gradually deceases with increasing [EtOH] revealing destabilization of the miceller aggre-gates. In contrast to the effect of urea, at higher concentration of the copolymers similar trend is also observed (Fig. 5(b)). However, for SAVal-DA(0.16) copolymer, the change of r is small, which con-firms tighter packing of the hydrocarbon chains in the aggregate at higher concentration.

The effect of salt concentration on the stability of the copoly-mer micelles is shown by the plots of $\Delta\lambda$ of AN, and r-value of DPH as a function of [NaCl] in Fig. 6. For the copolymers, $\Delta\lambda$ grad-ually increases with the increase of [NaCl], reaching a plateau at
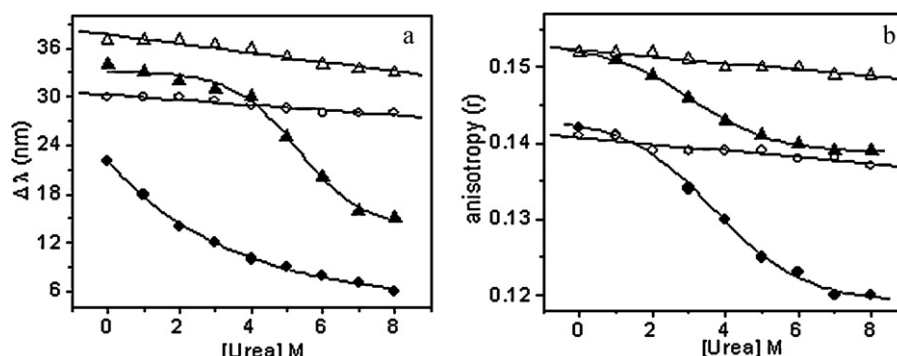

Fig. 3. (a) Plots of shift of emission maximum ($\Delta\lambda$) of AN as a function of [urea]; (b) plot fluorescence anisotropy (r) versus [urea] for 0.25 g/L (closed symbol) and 1.0 g/L (open symbol) SAVal-DA(0.09) (circle) and SAVal-DA(0.16) (triangle).
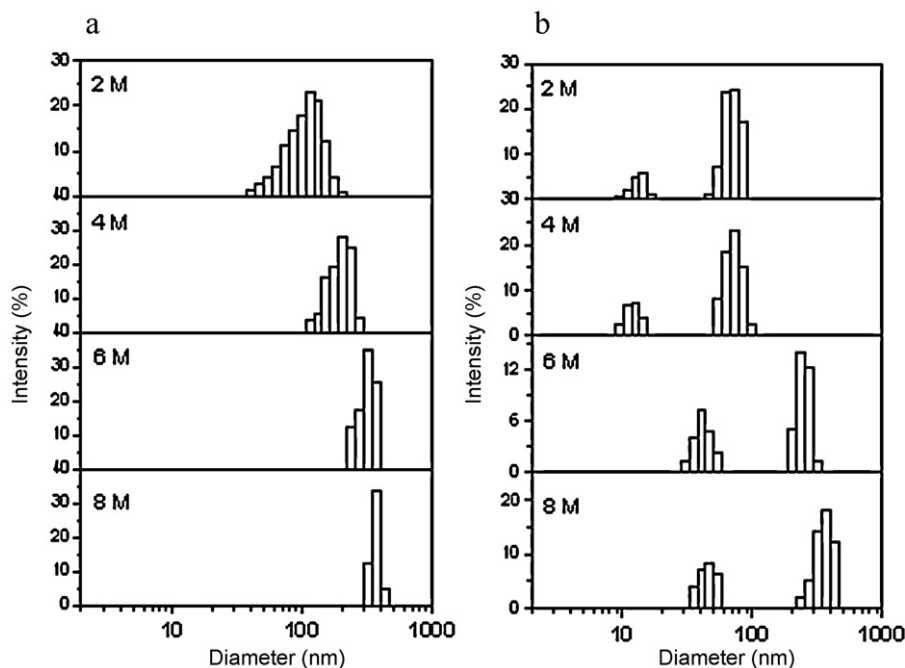
Fig. 4. Intensity average size distributions in 0.25 g/L (a) SAVal-DA(0.09) and (b) SAVal-DA(0.16) copolymer solutions in the presence of different urea concentrations.
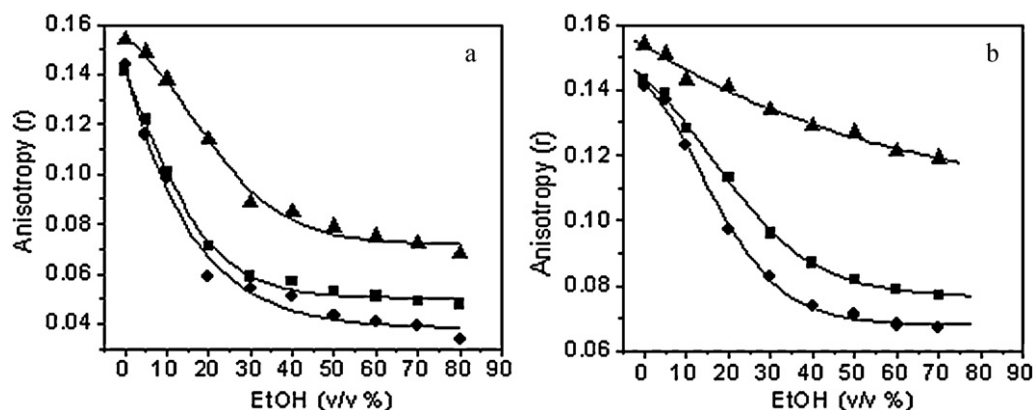

Fig. 5. Plots of fluorescence anisotropy (r) of DPH as a function of [EtOH] (v/v %) for (a) 0.25 g/L and (b) 1.0 g/L. (●) SAVal-DA(0.09), (■) SAVal-OA(0.16), and (▲) SAVal-DA(0.16) copolymers.
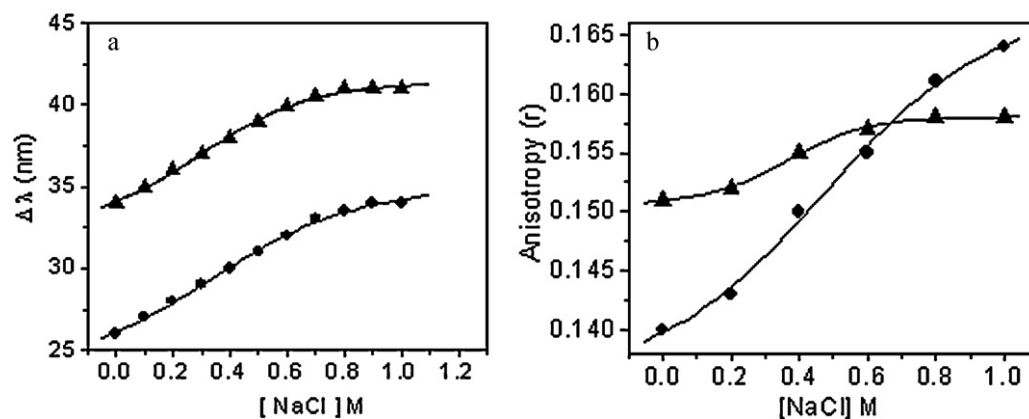

Fig. 6. Plots of (a) shift of emission maximum ($\Delta\lambda$) of AN versus [NaCl] and (b) anisotropy (r) of DPH versus [NaCl] in 0.25 g/L of the copolymers, (●) SAVal-DA(0.09) and (▲) SAVal-DA(0.16).
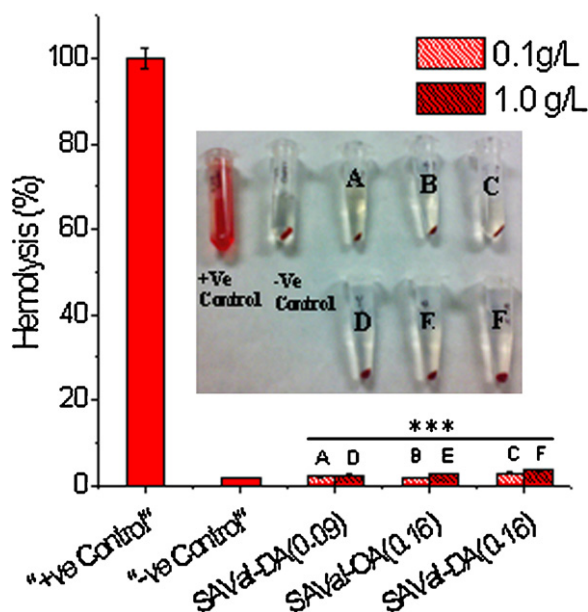
Fig. 7. Percentage of hemolysis of copolymers at 0.1 g/L and 1 g/L concentration at physiological pH (7.4). (Inset: the picture represents hemolytic assay of the copolymers.) Significant difference is shown as ***$p < 0.001$ versus +ve control. The bars indicate the means ± SD ($n = 3$).

Fig. 8. MTT assay based fibroblast cell line 3T3 cell viability (in %) as a function of concentration for copolymers at physiological pH (7.4). Significant difference is shown as ***$p < 0.001$ versus +ve control. The bars indicate the means ± SD ($n = 3$).

moderate ionic strength, reflecting collapse of the polymer chains into a compact globular like state. However, the increase is more pronounced in dilute polymer solution of the HMPs. Pronounced conformational change could also be observed with the copolymer SAVal-DA(0.09) with lower hydrophobe content. This is due to reduction of ionic repulsions among the negatively charged amino acid moieties in the polymer backbone. The increased r-value in the presence of high salt concentration also suggests salt-induced conformational transition to a more compact state. The salt-induced conformational transition is further indicated by the reduction of average R_h value of the aggregates of SAVal-DA(0.16) from 34 nm to 23 nm, and of SAVal-DA(0.09) from 62 nm to 44 nm upon addition of 0.8 M NaCl.

3.5. Hemocompatibility studies

To explore the compatibility of the copolymers with blood components, hemolytic assays were performed for all the three copolymers SAVal-DA(0.09), SAVal-DA(0.16), and SAVal-OA(0.16) in pH 7.4 (HEPES buffer, 20 mM). Freshly isolated BALB/c male mice red blood cell (RBC) suspension (5% v/v) was added to HEPES-buffered saline, 1% Triton X-100 and polymers with a final concentration of 0.01 and 1.0 g/L, and incubated for 60 min at 37 °C. The pictures associated to the hemolytic experiments are presented in inset of Fig. 7. As seen, clearly none of the samples exhibit any hemolysis.

To quantify the hemolytic activity of polymer samples for each treatment, the percentage of cell lysis relative to the untreated cell (% control) was determined by measuring the absorbance (570 nm) of the supernatant. Hemolytic activity (in %) of the copolymers along with the +ve and −ve control is presented in Fig. 7. It is known that any sample with less than 5% hemolysis ratio is regarded as nontoxic (Rao and Sharma, 1997). In the present investigation, it is observed that the copolymers SAVal-DA(0.09), SAVal-DA(0.16), and SAVal-OA(0.16) at a concentration of 0.1 g/L exhibit 2.1 ± 0.21, 1.8 ± 0.05, and 2.8 ± 0.11% hemolysis, respectively. Therefore, with hydrophobic substitution in the amino acid side chain of copolymers did not exhibit any significant lysis to RBC
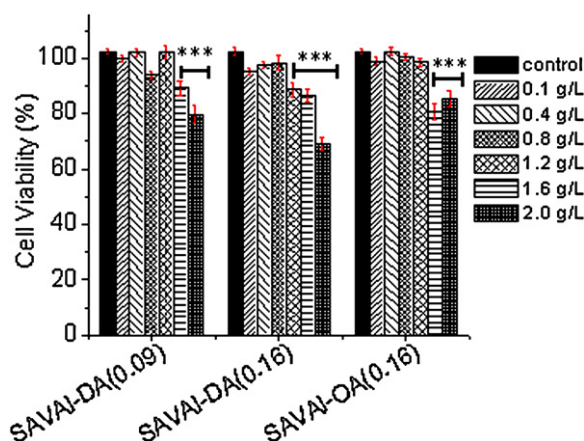
membrane and hemolytic activity of the copolymers was independent on the hydrophobic composition or hydrophobic chain length to poly(sodium N-acryloyl-L-valinate). When the final concentration was increased to 1.0 g/L, the hemolysis was found to increase to 2.5 ± 0.08, 2.7 ± 0.18, and 3.5 ± 0.13%, respectively. However, the values (<5%) still remain within the limit of toxicity. Hence, the copolymers are practically compatible to blood component RBC.

3.6. Cytotoxicity studies

The biocompatibility of the copolymers was also evaluated by measuring the toxicity on fibroblast cell line. The cytotoxicity of the copolymers in the concentration range of 0.1–2.0 g/L at physiological pH (7.4) was evaluated by measuring the viability of 3T3 cells using the MTT assay. The cell viability is shown in Fig. 8. The results exhibited insignificant amount of cell death at the concentration range of 0.1–2.0 g/L and more than 60% cells are still found viable which indicate cytocompatibility of the present copolymers under study.

4. Conclusions

In conclusion, we have investigated the solubilization capacities of three new class of micelle-forming L-amino acid-based hydrophobically modified anionic polymers, SAVal-DA(0.16), SAVal-OA(0.16), and SAVal-DA(0.09) for various prescription NSAID molecules that have poor aqueous solubility. The solubilities of the drugs were observed to increase linearly with the polymer concentration. In all the cases, depending upon the hydrophobicity of the molecules, solubility was found to increase ca. 2–10 times in the presence of 1.0 g/L copolymers. In any polymer solution of a given concentration (1 g/L), the equilibrium solubilities of the six NSAIDs (e.g., KTP, INP, FNP, FLP, NPX, and SUP) were observed to decrease in the order SUP > KTP > INP > NPX > FNP > FLP and for any of the drugs, the solubilities in the three polymer solutions increased in the order SAVal-DA(0.09) < SAVal-OA(0.16) < SAVal-DA(0.16). The large drug loading capacity of the polymers suggests potential application of the above-mentioned HMPs in drug delivery. These polymers when tested for pH and temperature-responsive in vitro release of two representative drug molecules, KTP and NPX, sustained release of the drugs over a period of 10–50 h was observed in presence of the copolymers at pH 5. However, at the physiological pH (7.4) the release was observed to be faster. The stability of the polymeric aggregates was studied under differ-

ent environmental conditions (e.g., salt concentration, and organic additives). Though, the aggregates become unstable upon addition of ethanol or urea, addition of increasing amount of NaCl was found to enhance stability of the aggregates. As evaluated by MTT assay with mammalian 3T3 cells, all the three anionic copolymers did not affect the growth of 3T3 cells. They were also found to pass the test for hemocompatibility. It is also important to note that large sizes (>40 nm) of the HMPs in combination with their high drug loading capacity can enhance bioavailability of the solubilized drug molecules.

Acknowledgements

References

Allen, T.M., Cullis, P.R., 2004. Drug delivery systems: entering the mainstream. Science 303, 1818–1822.

Cashion, M.P., Long, T.E., 2009. Biomimetic design and performance of polymerizable lipids. Acc. Chem. Res. 42, 1016–1025.

Cavalieri, F., Chiessi, E., Paradossi, G., 2007. Chaperone-like activity of nanoparticles of hydrophobized poly(vinyl alcohol). Soft Matter 3, 718–724.

Cevc, G., 1993. In: GregoriadisF G. (Ed.), Liposome Technology. , second ed. CRC, Boca Raton, FL, pp. 1–36.

Chelushkin, P.S., Lysenko, E.A., Bronich, T.K., et al., 2007. Polyion complex nanomaterials from block polyelectrolyte micelles and linear polyelectrolytes of opposite charge: 1. Solution behavior. J. Phys. Chem. B 111, 8419–8425.

Cortesi, R., Nastruzzi, C., 1999. Liposomes, micelles and microemulsions as a new delivery system for cytotoxic alkaloids. Pharm. Sci. Technol. Today 2, 288–298.

Deen, G.R., Gan, L.H., 2009. New piperazine-based polymerizable monoquaternary cationic surfactants: synthesis, polymerization, and swelling characteristics of gels. J. Polym. Sci. A: Polym. Chem. 47, 2059–2072.

Dutta, P., Dey, J., Ghosh, G., Nayak, R.R., 2009a. Self-association and microenvironment of random amphiphilic copolymers of sodium N-acryloyl-L-valinate and N-dodecylacrylamide in aqueous solution. Polymer 50, 1516–1525.

Dutta, P., Shrivastava, S., Dey, J., 2009b. Amphiphilic polymer nanoparticles: characterization and assessment as new drug carrier. Macromol. Biosci. 9, 1116–1126.

Elvira, C., Mano, J.F., San Román, J., Reis, R.L., 2002. Starch-based biodegradable hydrogels with potential biomedical applications as drug delivery systems. Biomaterials 23, 1955–1966.

Fan, Y., Han, Y., Wang, Y., 2007. Solubilization of phosphatidylcholine vesicles by hydrophobically modified poly(acrylamide)-co-(acrylic acid): effects of acrylic acid fraction and polymer concentration. J. Phys. Chem. B 111, 10123–10129.

Farokhzad, O.C., Langer, R., 2009. Impact of nanotechnology on drug delivery. ACS Nano 3, 16–20.

Fini, A., Fazio, G., Feroci, G., 1995. Solubility and solubilization properties of nonsteroidal anti-inflammatory drugs. Int. J. Pharm. 126, 95–102.

Florence, A.T., Attwood, D., 1998. Physicochemical Principles of Pharmacy, Third ed. Macmillan Press, U.K, pp. 5–35.

Gao, W.-P., Bai, Y., Chen, E.-Q., et al., 2006. Controlling vesicle formation via interpolymer hydrogen-bonding complexation between poly(ethylene oxide)-block-polydutadiene and poly(acrylic acid) in solution. Macromolecules 39, 4894–4898.

Garnier, S., Laschewsky, A., 2006. New amphiphilic diblock copolymers: surfactant properties and solubilization in their micelles. Langmuir 39, 4044–4053.

Guo, W., Huang, K., Tang, R., Xu, H., 2005. Synthesis, characterization of novel injectable drug carriers and the antitumor efficacy in mice bearing sarcoma-180 tumor. J. Control. Release 107, 513–522.

Gupta, S., Moulik, S.P., 2008. Biocompatible microemulsions and their prospective uses in drug delivery. J. Pharm. Sci. 97, 22–45.

Hadgraft, J., Plessis, J., Goosen, C., 2000. The selection of non-steroidal anti-inflammatory agents for dermal delivery. J. Pharm. Sci. 207, 31–37.

Hua, F., Jiang, X., Zhao, B., 2006. Temperature-induced self-association of doubly thermosensitive biblock copolymers with pendant methoxytris(oxyethylene) groups in dilute aqueous solution. Macromolecules 39, 3476–3479.

Kakinoki, S., Taguchi, T., Satio, H., Tanaka, J., 2007. Injectable in situ forming drug delivery system for cancer chemotherapy using a novel tissue adhesive: characterization and in vitro evaluation. Eur. J. Pharm. Biopharm. 66, 383–390.

Kantaria, S., Rees, G.D., Lawrence, M.J., 1999. Gelatin based organogels: rheology and application in ionophoretic transdermal drug delivery. J. Contr. Del. 60, 355–365.

Katanasaka, Y., Ida, T., Asai, T., Shimizu, K., Koizumi, F., Maeda, N., Baba, K., Oku, N., 2008. Antiangiogenic cancer therapy using tumor vasculature-targeted liposomes encapsulating 3-(3,5-dimethyl-1H-pyrrol-2-ylmethylene)-1,3-dihydro-indol-2-one, SU5416. Cancer Lett. 270, 260–268.

Khatua, D., Dey, J., 2007. Fluorescence, circular dichroism, light scattering, and microscopic characterization of vesicles of sodium salts of three N-acyl peptides. J. Phys. Chem. B 111, 124–130.

Klaikherd, A., Nagamani, C., Thayumanavan, S., 2009. Multi-stimuli sensitive amphiphilic block copolymer assemblies. J. Am. Chem. Soc. 131, 4830–4838.

Kreuter, J., 1994. Nanoparticles. In: Kreuter, J. (Ed.), Colloidal Drug Delivery Systems. Marcel Dekker, New York, pp. 219–342.

Kunze, A., Svedhem, S., Kasemo, B., 2009. Lipid transfer between charged supported lipid bilayers and oppositely charged vesicles. Langmuir 25, 5146–5158.

Kujawa, P., Tanaka, F., Winnik, F.M., 2006. Temperature-dependent properties of telechelic hydrophobically modified poly(N isopropylacrylamides) in water: evidence from light scattering and fluorescence spectroscopy for the formation of stable mesoglobules at elevated temperatures. Macromolecules 39, 3048–3055.

Lawrence, M.J., 1996. Microemulsions as drug delivery vehicles. Curr. Opin. Colloid Interface Sci. 1, 826–832.

Leo, A., Hansch, C., Elkins, D., 1971. Partition coefficients and their uses. Chem. Rev. 71, 525–616.

Liu, R.C.W., Pallier, A., Brestaz, M., Pantoustier, N., Tribet, C., 2007. Impact of polymer microstructure on the self-assembly of amphiphilic polymers in aqueous solutions. Macromolecules 40, 4276–4286.

Liu, Z., Zhang, Z., Zhou, C., Jiao, Y., 2010. Hydrophobic modifications of cationic polymers for gene delivery. Prog. Polym. Sci. 35, 1144–1162.

Maeda, H., Wu, J., Sawa, T., Matsumura, Y., Hori, K., 2000. Tumor vascular permeability and the EPR effect in macromolecular therapeutics: a review. J. Control. Release 65, 271–284.

Makiko, F., Naohide, H., Kumi, S., 2000. Effect of fatty acid esters on permeation of ketoprofen through hairless rat skin. Int. J. Pharm. 205, 117–125.

Marie, R.G., 1998. Epidemiology of nonsteroidal anti-inflammatory drug-associated gastrointestinal injury. Am. J. Med. 104, 23S–29S.

Miguel, V.S., Limer, A.J., Haddleton, D.M., Catalina, F., Peinado, C., 2008. Biodegradable and thermoresponsive micelles of triblock copolymers based on 2-(N,N-dimethylamino)ethyl methacrylate and ε-caprolactone for controlled drug delivery. Eur. Polym. J. 44, 3853–3863.

Min, K.H., Park, K., Kim, Y.S., Bae, S.M., Lee, S., Jo, H.G., Park, R.W., Kim, I.S., Jeong, S.Y., Kim, K., Kwon, I.C., 2008. Hydrophobically modified glycol chitosan nanoparticles-encapsulated camptothecin enhance the drug stability and tumor targeting in cancer therapy. J. Control. Release 127, 208–218.

Moulik, S.P., Paul, B.K., 1998. Structure, dynamics and transport properties of microemulsions. Adv. Colloid Interface Sci. 78, 99–195.

Obeid, R., Maltseva, E., Thunemann, A.F., Tanaka, F., Winnik, F.M., 2009. Temperature response of self-assembled micelles of telechelic hydrophobically modified poly(2-alkyl-2-oxazoline)s in water. Macromolecules 42, 2204–2214.

Okino, H., Nakayama, Y., Tanaka, M., Masuda, T., 2002. In situ hydrogelation of photocurable gelatin and drug release. J. Biomed. Mater. Res. 59, 233–245.

Péhourcq, F., Matoga, M., Jarry, C., Bannwarth, B., 2001. Study of the lipophilicity of arylpropionic non-steroidal anti-inflammatory drugs: a comparison between LC retention data on a polymer-based column and octanol water partition coefficients. J. Liq. Chromatogr. Relat. Technol. 24, 2177–2186.

Rao, S.B., Sharma, C.P., 1997. Use of chitosan as a biomaterial: studies on its safety and hemostatic potential. J. Biomed. Mater. Res. 34, 21–28.

Reddy, H.L., Vivek, K., Bakshi, N., Murthy, R.S.R., 2006. Tamoxifen citrate loaded solid lipid nanoparticles(SLN™): preparation, characterization, in vitro drug release, and pharmacokinetic evaluation. Pharm. Dev. Technol. 11, 167–177.

Repáková, J., Eapková, P., Holopainen, J.M., Vattulainen, I., 2004. Distribution, orientation, and dynamics of DPH probes in DPPC bilayer. J. Phys. Chem. B 108, 13438–13448.

Ritger, P.L., Peppas, N.A., 1987. A simple equation for description of solute release. I. Fickian and non-fickian release from non-swellable devices in the form of slabs, spheres, cylinders or discs. J. Control. Release 5, 23–36.

Sakai, K., Wada, M., Matsuda, W., Tsuchiya, K., Takamatsu, Y., Tsubone, K., Endo, T., Torigoe, K., Sakai, H., Abe, M., 2009. Polymerizable anionic gemini surfactants: physicochemical properties in aqueous solution and polymerization behavior. J. Oleo Sci. 58, 403–413.

Tenjarala, S., 1999. Microemulsions: an overview and pharmaceutical applications. Crit. Rev. Ther. Drug Carrier Syst. 16, 461–521.

Torchilin, V.P., 2001. Structure and design of polymeric surfactant-based drug delivery systems. J. Control. Release 73, 137–172.

Uchegbu, F., Florence, A.T., 1995. Non-ionic surfactant vesicles (niosomes): physical and pharmaceutical chemistry. Adv. Colloid Interface Sci. 58, 1–55.

Watnasirichikul, S.S., Davis, N.M., Rades, T., Tucker, I.G., 2002. Preparation of biodegradable insulin nanocapsules from biocompatible microemulsions. Pharm. Res. 17, 684–689.

Wittemann, A., Azzam, T., Eisenberg, A., 2007. Biocompatible polymer vesicles from biamphiphilic triblock copolymers and their interaction with bovine serum albumin. Langmuir 23, 2224–2230.

Yalkowsky, S.H., 1999. Solubility and Solubilization in Aqueous Media. Oxford University Press, New York (Chapter 7).

Yang, J., Piñol, R., Gubellini, F., Lévy, D., Albouy, P.A., Keller, P., Li, M.H., 2006. Formation of polymer vesicles by liquid crystal amphiphilic block copolymers. Langmuir 22, 7907–7911.

Yiyun, C., Tongwen, X., 2005. Dendrimers as potential drug carriers. Part I. Solubilization of non steroidal anti-inflammatory drugs in the presence of polyamidoamine dendrimers. Eur. J. Med. Chem. 40, 1188–1192.

Yumiko, N., Kozo, T., Kimio, H., 1996. Promoting effect of O-ethylmenthol on the percutaneous absorption of ketoprofen. Int. J. Pharm. 145, 29–36.